

Equivalent Circuit for Magnetoelectric Read and Write Operations

Kerem Y. Camsari,¹ Rafatul Faria,¹ Orchi Hassan,¹ Brian M. Sutton,¹ and Supriyo Datta¹

¹*School of Electrical and Computer Engineering, Purdue University, IN, 47907*

(Dated: April 18, 2018)

We describe an equivalent circuit model applicable to a wide variety of magnetoelectric phenomena and use SPICE simulations to benchmark this model against experimental data. We use this model to suggest a different mode of operation where the “1” and “0” states are not represented by states with net magnetization (like m_x , m_y or m_z) but by different easy axes, quantitatively described by $(m_x^2 - m_y^2)$ which switches from “0” to “1” through the write voltage. This change is directly detected as a read signal through the inverse effect. The use of $(m_x^2 - m_y^2)$ to represent a bit is a radical departure from the standard convention of using the magnetization (m) to represent information. We then show how the equivalent circuit can be used to build a device exhibiting tunable randomness and suggest possibilities for extending it to non-volatile memory with read and write capabilities, without the use of external magnetic fields or magnetic tunnel junctions.

I. INTRODUCTION

In magnetic random access memory (MRAM) technology write units are typically based on spin-torque or spin-orbit torque, while read operations are based on the magnetoresistance of magnetic tunnel junctions (MTJ). But there is increasing interest in voltage-driven units due to the potential for low power operation, both active and stand-by based on different types of magnetoelectric phenomena [1–20].

The central result of this paper is an equivalent circuit model (Fig. 1) applicable to a range of magnetoelectric (ME) phenomena including both write and read operations. It consists of a capacitor circuit which incorporates the back voltage from the magnetoelectric coupling described by (1):

$$V_{\text{IN}} = \frac{Q}{C_L} + \frac{Q}{C} + \frac{\partial E_m}{\partial Q} \quad (1)$$

where E_m is the magnetic energy including the part controlled by the charge Q on an adjacent capacitor C , through the ME effect. Equation (1) is solved self-consistently with the stochastic Landau-Lifshitz-Gilbert (s-LLG) equation which feels an effective field ($\vec{H}_{me} = -\nabla_{\mathbf{m}} E_m / \{M_s \text{Vol.}\}$), $\nabla_{\mathbf{m}}$ represents the gradient operator with respect to magnetization directions \hat{m}_i , M_s is the saturation magnetization and Vol. is the volume of the magnet. The s-LLG treatment for all simulations in this paper is similar to what is described in [21–23] and is not repeated here. We first benchmark this equivalent circuit against the recently demonstrated MagnetoElectric Random Access Memory (MELRAM) device [24, 25] which uses the magnetoelectric effect (ME) and its inverse (IME) for write and read operations, using a structure whose energy E_m is given by Eq. 2. We then argue that, unlike MELRAM, the “1” and the “0” states need not be represented by states with a net magnetization. For example, using a structure whose energy E_m is given by Eq. 4, one could instead switch the easy axis with a write voltage, and this change in the easy axis can be

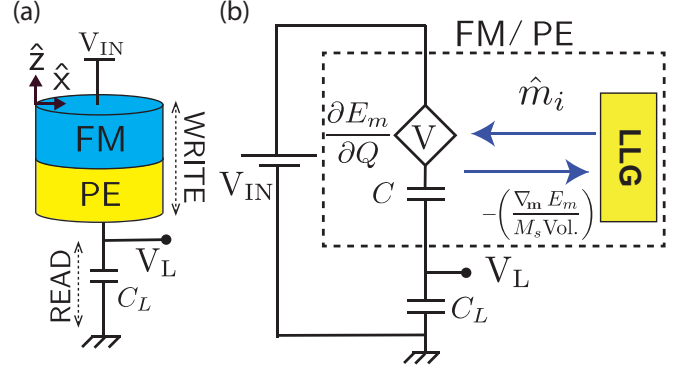


Fig. 1. Equivalent circuit for magnetoelectric (ME) read and write operations (a) The charge on the piezoelectric (PE) capacitor changes the easy-axis of the ferromagnet (FM) and this causes a change in the output voltage V_L through the inverse effect. (b) Equivalent circuit model obtained from (1). Write operation is through the effective field $\vec{H}_{me} = -\nabla_{\mathbf{m}} E_m / (M_s \text{Vol.})$ that enters the stochastic Landau-Lifshitz-Gilbert (s-LLG) equation. Read operation is through the dependent voltage source V that is proportional to $\partial E_m / \partial Q$, where E_m is the magnetic energy.

read as a change in the voltage across a series capacitor through the inverse effect, allowing a “field-free” operation without any symmetry breaking magnetic field.

II. EXPERIMENTAL BENCHMARK

We start with the MELRAM device (Fig. 2b) reported recently in [25] where the magnetic energy has the form

$$E_m = -E_A m_x m_y + E_H / \sqrt{2} (m_x - m_y) + v_M Q (m_x^2 - m_y^2) \quad (2)$$

We note that this energy expression is essentially the same as what was reported in Ref. [25] expressed using magnetization components, m_x, m_y, m_z . For example, the anisotropy energy is written in [25] as $-E_A \sin^2 \phi$,

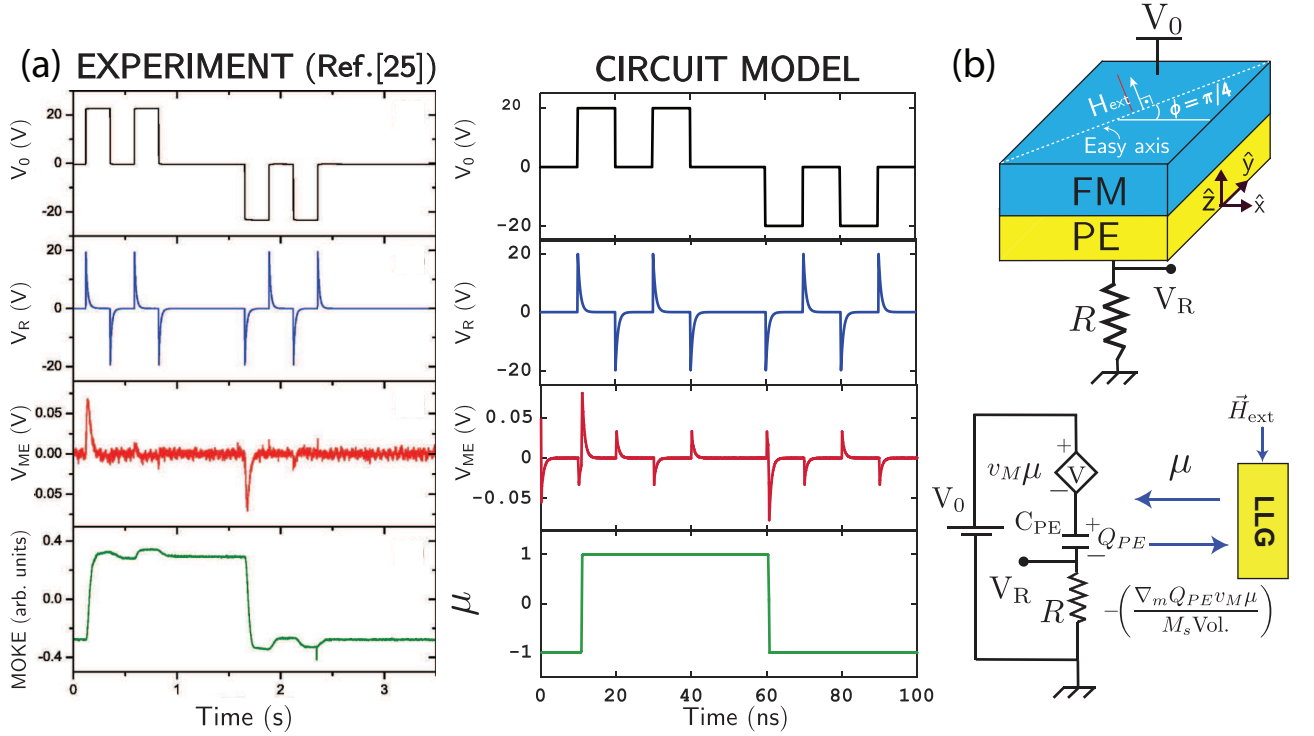


Fig. 2. Experiment vs circuit model: (a) The results of the self-consistent circuit model for the structure in (b) are in good agreement with the experimental results in [25]. V_{ME} is the mathematical difference of two measurements of V_R with and without the external magnetic field, $V_{ME} = V_R(H \neq 0) - V_R(H = 0)$. (b) Experimental structure reported in [25] where the piezoelectric (PE) is (011)-cut PMN-PT and the ferromagnet (FM) is N layers of TbCo₂/FeCo. The back-voltage is $V = v_M \mu$ where $\mu = m_x^2 - m_y^2$ and the magnetic energy is $E_m = Q_{PE} v_M \mu$ where Q_{PE} is the charge on the capacitor C_{PE} . The following parameters are used: Coercivity for FM ($H_K = 200$ Oe), saturation magnetization $M_s = 1100$ emu/cc, FM thickness, $t_{FM} = 200$ nm, PE thickness $t_{PE} = 30$ μ m, Area = 520×520 nm², Magnetoelastic constant $B = -7$ MPa, a net PE constant, $d = d_{31} - d_{32} = 2500$ pC/N, permittivity $\epsilon = 4033 \epsilon_0$, resistance $R = 2$ M Ω , back voltage $v_M = B d_{FM} / 2\epsilon$. In the experiment, magneto-optic Kerr effect (M.O.K.E) is used to show the variation of magnetization, which is compared to the pseudo-magnetization in our simulation. Experimental panel is reproduced with permission of AIP Publishing LLC, from Reference [25].

with ϕ measured from the magnetic field \vec{H}_{ext} such that $m_x = \cos(3\pi/4 - \phi)$, $m_y = \sin(\pi/4 - \phi)$ and $m_x m_y = \sin^2 \phi$, ignoring an unimportant constant. Similarly the Zeeman term is written in [25] as $-E_H \cos \phi$ which equals $E_H(m_x - m_y)/\sqrt{2}$. In [25], the uniaxial anisotropy energy term and the external magnetic field were ingeniously balanced (by choosing $E_H = E_A \sqrt{2}$) to provide two unique low energy states that represent “0” and “1” at $\phi = \pi/2$ and $\phi = \pi$.

Finally, the last term represents the ME effect where an applied voltage generates a charge Q , controlled by the input voltage V_{IN} , which changes the anisotropy energy such that a positive (or negative) Q causes the magnetic energy to favor the y-axis (or the x-axis) for a positive v_M . This is due to the anisotropic piezoelectric coefficients d_{31} and d_{32} having different signs, a special property of the (011)-cut (PMN-PT) that was chosen in the experiment.

The equivalent circuit incorporates the back voltage from the ME coupling using (1), with the load capacitor

C_L replaced by a resistor R :

$$\begin{aligned} V_{IN} &= R \frac{dQ}{dt} + \frac{Q}{C} + \frac{\partial E_m}{\partial Q} \\ &= R \frac{dQ}{dt} + \frac{Q}{C} + v_M(m_x^2 - m_y^2) \end{aligned} \quad (3)$$

It is possible to write the ME energy as $q_M V$ in terms of an applied voltage V rather than charge Q , but this choice would lead to a back charge $\partial E_m / \partial V$ instead of a back voltage $\partial E_m / \partial Q$, giving a different but equivalent looking circuit model.

Fig. 2a shows the write and read signals for the experimental structure in Fig. 2b calculated using a SPICE model, that are in good agreement with the experimental results presented in [25]. The reason for the very different time scales of the experiment and the circuit model is that the circuit model solves the real-time dynamics of the nanomagnet with time steps of the order of a fraction of the inverse FMR frequency of the nanomagnet ($1/f \sim 2\pi/\gamma/\sqrt{[H_K(H_K + 4\pi M_s)]} \sim 0.2$ ns for the

chosen parameters) to avoid large numerical integrations while the experimental measurement is performed with quasi-static pulses. Therefore the RC time constants in both cases are very different, however the maxima and minima of each signal closely match based on the chosen parameters.

III. FIELD-FREE OPERATION

It is evident from Fig. 2a that our equivalent circuit describes the switching process accurately in the experiment described in Ref. [25]. Using the same circuit model we would like to suggest the possibility of field-free operation where “0” and “1” are represented by two different easy axes rather than two different magnetization directions. For this illustration, we consider a ferromagnet whose easy axis does not lie along $m_x = \pm m_y$ as in Ref. [25], but rather along the y-axis ($m_x = 0$), corresponding to an anisotropy energy given by $E_A(m_x^2 - m_y^2)$. Also, there is no external magnetic field so that $E_H = 0$ giving an overall energy expression of the form

$$E_m = (E_A + v_M Q)(m_x^2 - m_y^2) \quad (4)$$

instead of Eq. 2.

A positive induced charge Q makes y -direction the easy axis so that $\langle m_x^2 - m_y^2 \rangle = -1$, while a negative Q makes x -direction the easy axis so that $\langle m_x^2 - m_y^2 \rangle = +1$, and this constitutes the writing operation. The inverse of the same effect gives rise to a back voltage that allows one to read the information. Using (4) we obtain from (1):

$$V_{IN} = \frac{Q}{C_L} + \frac{Q}{C} + v_M(m_x^2 - m_y^2) \quad (5)$$

Use of this “pseudo-magnetization” $\mu \equiv m_x^2 - m_y^2$ is a radical departure from the standard convention of using the magnetization (m_x, m_y or m_z) to represent a bit [26], opening up new possibilities for writing and reading.

Even though we have limited our discussion to the composite PE / FM structures that give rise to a magnetoelectric effect due to a coupling of the strain from a PE material to a magnetostrictive FM material, we believe the circuit description described in Fig. 1 could be of general use. Indeed, it should be possible to use other quantities represented by a function $f(m_x, m_y, m_z)$ to represent a bit. Any mediating term due to strain, charge, orbital or other microscopic mechanisms giving rise to a term of the form $(Q \times f)$ in the energy expression that can be used to write such a bit, should also give rise to an inverse effect for read out.

In the next two sections, we show two example uses of the external magnetic field-free operation of the equivalent circuit.

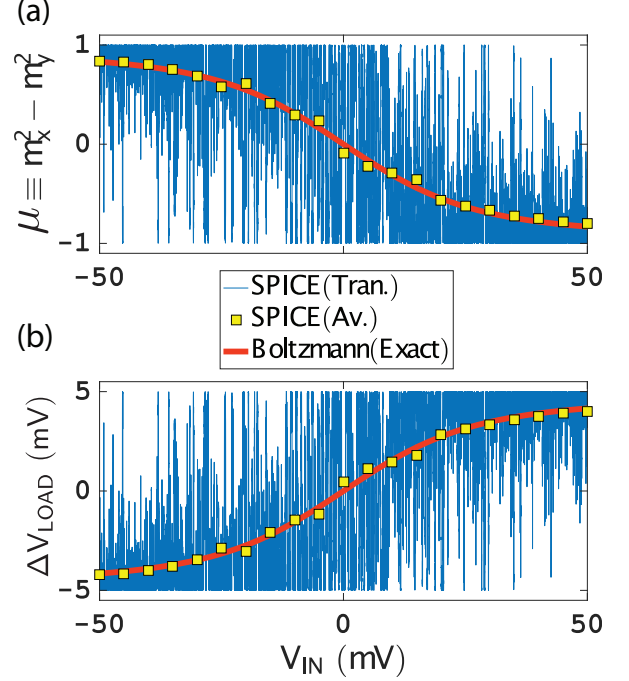


Fig. 3. Tunable randomness: Results for the structure in Fig. 1a using the circuit model in Fig. 1b with a circular magnet ($H_K \rightarrow 0, E_A \rightarrow 0$). $C = C_L = 50$ aF and $v_M = 10$ mV such that $C_{\text{eff}} v_M^2 / kT < 1$ (a) Three results are shown for magnetization, μ : Transient SPICE simulations (Solid blue) where the input voltage (V_{IN}) is swept from -50 mV to $+50$ mV in $1 \mu\text{s}$ and pseudo-magnetization, μ is plotted against V_{IN} . Separate SPICE simulations for each solid square where an average magnetization is obtained over 100 ns. Exact Boltzmann integral obtained from Eq. 6. (b) Same results for the differential load voltage, $\Delta V_L = V_L - V_L(v_M = 0)$, in this case $V_L(v_M = 0) = V_{IN}/2$. The actual load voltage has a linear V_{IN} dependence superimposed on ΔV_L , similar to Fig. 4. The differential load voltage is shown here for clarity.

IV. EXAMPLE #1: TUNABLE RANDOMNESS

The first example we illustrate using the equivalent circuit of Fig. 1 is obtained by coupling the circuit shown in Fig. 1 with a low-barrier circular nanomagnet that does not have an easy axis ($H_K \rightarrow 0$) and no energy barrier ($E_A = 0$) that favors a magnetization axis [27, 28]. The magnetization of such a magnet fluctuates randomly in the plane, in the presence of thermal noise. The read and write mechanisms of the ME effect convert the fluctuations in the pseudo-magnetization μ to a voltage.

Fig. 3 shows the differential load voltage ΔV_L vs V_{IN} assuming $C = C_L = 50$ aF making $C_{\text{eff}} = CC_L / (C + C_L) = 25$ aF and $v_M = 10$ mV, consistent with the material parameters for the experimental system in Fig. 2b, though the coupling coefficient v_M is chosen somewhat smaller, (such that $C_{\text{eff}} v_M^2 / kT < 1$, as we explain in the next section) in order to avoid any hysteresis or memory effects. Alternatively one could use a smaller load

capacitance, reducing C_{eff} .

With this choice of parameters, the magnetizations and hence the voltages fluctuate with time, and the averaged values over a time interval of ≈ 100 ns match the average results obtained from the Boltzmann probability:

$$\langle \mu \rangle = \frac{\int_{Q=-\infty}^{Q=+\infty} \int_{\phi=-\pi}^{\phi=+\pi} d\phi dQ \overbrace{\cos(2\phi)}^{\mu=m_x^2-m_y^2} \rho(Q, \phi)}{\int_{Q=-\infty}^{Q=+\infty} \int_{\phi=-\pi}^{\phi=+\pi} d\phi dQ \rho(Q, \phi)} \quad (6)$$

where $\rho(Q, \phi) = 1/Z \exp[-E(\phi, Q)/kT]$ and $E = Qv_M\mu + Q^2/(2C_{\text{eff}}) - QV_{\text{IN}}$ represents the total energy. Similar to our previous discussion, we assume that the magnetization for the circular in-plane magnet is confined to the plane of the magnet due to the strong demagnetization field. Therefore, the magnetization integral can be taken in the plane ($\phi \rightarrow \pm\pi$) and this seems to be in good agreement with the numerical s-LLG results as shown in Fig. 3. The average load voltage is obtained using Eq. 6, but replacing $\cos(2\phi)$ with Q/C_L .

Eq. 6 does not seem to reduce to a compact closed form, but assuming $Q = C_{\text{eff}}(V_{\text{IN}} \pm v_M|\mu|) \approx C_{\text{eff}}V_{\text{IN}}$ for small v_M , allows a direct evaluation:

$$\langle \mu \rangle \approx -\frac{I_1(x)}{I_0(x)} \quad (7)$$

where I_n is the modified Bessel function of the first kind [29], and $x = Qv_M/kT$. This approximation (not shown) seems to be in good agreement with an exact numerical evaluation of Eq. 6 that is shown in Fig. 3 and could be useful as an analytical guide.

Note that the SPICE simulation solves the magnetization and the load voltage self-consistently following the equivalent circuit (Fig. 1a) while the Boltzmann law takes these self-consistencies into account exactly. The agreement between the two constitutes another important benchmark for our equivalent circuit.

With additional gain and isolation that can be incorporated by CMOS components this field-free voltage-tunable randomness can become a potential voltage controllable “p-bit” (probabilistic bit) that can be used as a building block for a new type of probabilistic logic [30–35] or other neuromorphic approaches that make use of stochastic units [36–41], but this is not discussed further.

V. EXAMPLE #2: NON-VOLATILE OPERATION

It is easy to see by integrating Eq. 6 that even when one uses a stable magnet ($E_A > 40$ kT) in Eq. 4, the pseudo-magnetization μ does not show “hysteretic” behavior as function of V_{IN} , but simply shifts the sigmoidal response of Fig. 3 to the left or right depending on the

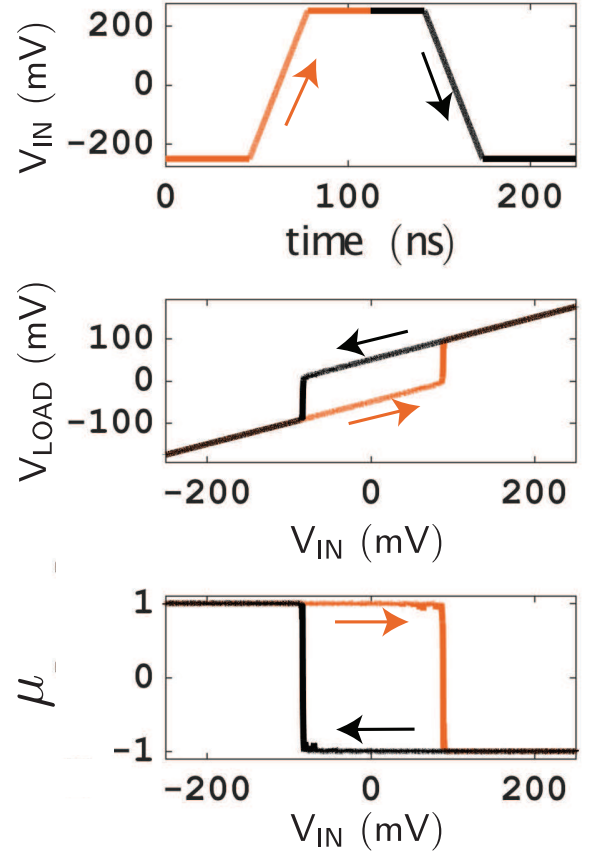


Fig. 4. Non-volatility: When $C_{\text{eff}}v_M^2/kT$ exceeds 1, the pseudo-magnetization (μ) for the circular magnet ($H_K \rightarrow 0, E_A \rightarrow 0$) investigated in Fig. 3 becomes stable. (a) Shows the input voltage (V_{IN}) doing a negative-positive-negative sweep as a function of time. (b) Load voltage ($C = C_L = 100$ aF) as a function of V_{IN} . (c) μ as a function of V_{IN} , exhibiting hysteresis.

sign of E_A . The average sigmoidal behavior of Fig. 3 is not just a consequence of using circular magnets, even a 40 kT magnet would show non-hysteretic behavior, but with suppressed fluctuations in μ and a shift along the V_{IN} axis. To obtain hysteretic behavior for the pseudo-magnetization μ we need an energy term that is quadratic ($\sim \mu^2$) rather than linear ($= E_A \mu$) as in Eq. 4, but we will not discuss the possibility further in this paper. Next we show that the energy expression we have used could lead to hysteretic behavior if the ME coefficient v_M were large enough. Such a quadratic term could arise naturally from the physics which we hope motivates future investigation.

Fig. 4 shows the results of a transient simulation of the equivalent circuit with a circular magnet, similar to Fig. 3 with the only difference that in this example the back-voltage (v_M) is increased to 100 mV such that $C_{\text{eff}}v_M^2/kT \gg 1$. An input voltage is slowly swept from -200 mV to +200 mV and back to -200 mV within 1

μ s, where pseudo-magnetization (μ) and the load voltage (V_L) show hysteresis, similar to the magnetization of an ordinary magnet. One way to understand the hysteretic behavior is to note that the total energy for the full circuit in Fig. 1 can be written as:

$$E_{total} = \frac{Q^2}{2C_{eff}} + Qv_M\mu - QV_{IN} \quad (8)$$

where $C_{eff}^{-1} = C^{-1} + C_L^{-1}$.

Expanding Eq. 7 for small v_M , we can approximate the pseudo-magnetization by $\mu \approx -Qv_M/(2kT)$ and we have:

$$E_{total} \approx \frac{Q^2}{2C_{eff}} - \frac{Q^2v_M^2}{2kT} - QV_{IN} \quad (9)$$

suggesting that the ME effect provides a *negative capacitance* $-kT/v_M^2$ in series with C_{eff} leading to hysteretic behavior when $C_{eff}v_M^2 > kT$ reminiscent of similar behavior based on ferroelectrics [42, 43].

Numerical simulations of the equilibrium fluctuations of this magnet also show that the thermal stability of the μ is $\approx C_{eff}v_M^2/kT$ which can be 60 or greater, for reasonable values of v_M and C_{eff} providing the possibility of non-volatile memory applications based on the pseudo-magnetization μ .

VI. CONCLUSION

In summary, we have presented an equivalent circuit for magnetoelectric read and write and showed that it describes recent experiments on the MELRAM device quite accurately. We then used this circuit model to illustrate the possibility of representing “1” with different easy axes, encoded by the pseudo-magnetization μ , rather than with different magnetizations, allowing a natural field-free operation that can be useful for a number of applications in stochastic neuromorphic computing. Lastly, we showed the possibility of using the pseudo-magnetization for non-volatile memory applications.

ACKNOWLEDGMENT

The authors acknowledge insightful discussions with V. Ostwal, P. Debashis, Z. Chen, J. Appenzeller, S. Majetich and J. T. Heron. This work was supported in part by the National Science Foundation through the NCN-NEEDS program, contract 1227020-EEC, the Nanoelectronics Research Initiative through the Institute for Nanoelectronics Discovery and Exploration (INDEX).

demonstration of complete 180° reversal of magnetization in isolated Co nanomagnets on a pmn-pt substrate with voltage generated strain,” Nano Letters (2017).

- [2] Kuntal Roy, Supriyo Bandyopadhyay, and Jayasimha Atulasimha, “Hybrid spintronics and straintronics: A magnetic technology for ultra low energy computing and signal processing,” Applied Physics Letters **99**, 063108 (2011).
- [3] Nickvash Kani, John T Heron, and Azad Naeemi, “Strain-mediated magnetization reversal through spin-transfer torque,” IEEE Transactions on Magnetics (2017).
- [4] Akhilesh Jaiswal and Kaushik Roy, “Mesl: Proposal for a non-volatile cascable magneto-electric spin logic,” Scientific reports **7** (2017).
- [5] Sasikanth Manipatruni, Dmitri E Nikonov, and Ian A Young, “Spin-orbit logic with magnetoelectric nodes: A scalable charge mediated nonvolatile spintronic logic,” arXiv preprint arXiv:1512.05428 (2015).
- [6] Tieren Gao, Xiaohang Zhang, William Ratcliff, Shingo Maruyama, Makoto Murakami, Anbusathiah Varatharajan, Zahra Yamani, Peijie Chen, Ke Wang, Huairuo Zhang, *et al.*, “Electric-field induced reversible switching of the magnetic easy axis in Co/BiFeO₃ on SrTiO₃,” Nano Letters **17**, 2825–2832 (2017).
- [7] JT Heron, JL Bosse, Q He, Y Gao, M Trassin, L Ye, JD Clarkson, C Wang, Jian Liu, S Salahuddin, *et al.*, “Deterministic switching of ferromagnetism at room temperature using an electric field,” Nature **516**, 370 (2014).
- [8] Xi He, Yi Wang, Ning Wu, Anthony N Caruso, Elio Vescovo, Kirill D Belashchenko, Peter A Dowben, and Christian Binek, “Robust isothermal electric control of exchange bias at room temperature,” Nature materials **9**, 579–585 (2010).
- [9] Zhengyang Zhao, Will Echtenkamp, Mike Street, Christian Binek, and Jian-Ping Wang, “Magnetoelectric device feasibility demonstration—voltage control of exchange bias in perpendicular Cr₂O₃/3 hall bar device,” in *Device Research Conference (DRC), 2016 74th Annual* (IEEE, 2016) pp. 1–2.
- [10] Pedram Khalili Amiri and Kang L Wang, “Voltage-controlled magnetic anisotropy in spintronic devices,” in *Spin*, Vol. 2 (World Scientific, 2012) p. 1240002.
- [11] Diana Chien, Xiang Li, Kin Wong, Mark A Zurbuchen, Shauna Robbennolt, Guoqiang Yu, Sarah Tolbert, Nicholas Kiousis, Pedram Khalili Amiri, Kang L Wang, *et al.*, “Enhanced voltage-controlled magnetic anisotropy in magnetic tunnel junctions with an mgo/pzt/mgo tunnel barrier,” Applied Physics Letters **108**, 112402 (2016).
- [12] Stephan K Piotrowski, Mukund Bapna, Samuel D Oberdick, Sara A Majetich, Mingen Li, CL Chien, Rizvi Ahmed, and RH Victora, “Size and voltage dependence of effective anisotropy in sub-100-nm perpendicular magnetic tunnel junctions,” Physical Review B **94**, 014404 (2016).
- [13] Meghna G Mankalale, Zhaoxin Liang, Zhengyang Zhao, Chris H Kim, Jian-Ping Wang, and Sachin S Sapatnekar, “Comet: Composite-input magnetoelectric-based logic technology,” IEEE Journal on Exploratory Solid-State Computational Devices and Circuits **3**, 27–36 (2017).
- [14] Asif Khan, Dmitri E Nikonov, Sasikanth Manipatruni, Tahir Ghani, and Ian A Young, “Voltage induced magnetostriuctive switching of nanomagnets: Strain assisted strain transfer torque random access memory,” Applied

[1] Ayan Kumar Biswas, Hasnain Ahmad, Jayasimha Atulasimha, and Supriyo Bandyopadhyay, “Experimental

- Physics Letters **104**, 262407 (2014).
- [15] NA Pertsev, "Giant magnetoelectric effect via strain-induced spin reorientation transitions in ferromagnetic films," *Physical Review B* **78**, 212102 (2008).
 - [16] Cheng Song, Bin Cui, Fan Li, Xiangjun Zhou, and Feng Pan, "Recent progress in voltage control of magnetism: Materials, mechanisms, and performance," *Progress in Materials Science* **87**, 33 – 82 (2017).
 - [17] Ren-Ci Peng, Jia-Mian Hu, Long-Qing Chen, and Ce-Wen Nan, "On the speed of piezostain-mediated voltage-driven perpendicular magnetization reversal: a computational elastodynamics-micromagnetic phase-field study," *NPG Asia Materials* **9**, e404 (2017).
 - [18] Jia-Mian Hu and C. W. Nan, "Electric-field-induced magnetic easy-axis reorientation in ferromagnetic/ferroelectric layered heterostructures," *Phys. Rev. B* **80**, 224416 (2009).
 - [19] Rouhollah Mousavi Iraei, Sourav Dutta, Sasikanth Manipatruni, Dmitri E Nikonov, Ian A Young, John T Heron, and Azad Naeemi, "A proposal for a magnetostriction-assisted all-spin logic device," in *Device Research Conference (DRC), 2017 75th Annual* (IEEE, 2017) pp. 1–2.
 - [20] Saima Sharmin, Yong Shim, and Kaushik Roy, "Magnetoelectric oxide based stochastic spin device towards solving combinatorial optimization problems," *Scientific Reports* **7** (2017).
 - [21] Jonathan Z Sun, "Spin-current interaction with a monodomain magnetic body: A model study," *Physical Review B* **62**, 570 (2000).
 - [22] Jonathan Z Sun, TS Kuan, JA Katine, and Roger H Koch, "Spin angular momentum transfer in a current-perpendicular spin-valve nanomagnet," in *Integrated Optoelectronic Devices 2004* (International Society for Optics and Photonics, 2004) pp. 445–455.
 - [23] Kerem Yunus Camsari, Samiran Ganguly, and Supriyo Datta, "Modular approach to spintronics," *Scientific reports* **5** (2015).
 - [24] Nicolas Tiercelin, Yannick Dusch, Alexey Klimov, Stefano Giordano, Vladimir Preobrazhensky, and Philippe Pernod, "Room temperature magnetoelectric memory cell using stress-mediated magnetoelastic switching in nanostructured multilayers," *Applied Physics Letters* **99**, 192507 (2011).
 - [25] Alexey Klimov, Nicolas Tiercelin, Yannick Dusch, Stefano Giordano, Théo Mathurin, Philippe Pernod, Vladimir Preobrazhensky, Anton Churbanov, and Sergei Nikitov, "Magnetoelectric write and read operations in a stress-mediated multiferroic memory cell," *Applied Physics Letters* **110**, 222401 (2017).
 - [26] Dmitri E Nikonov, Sasikanth Manipatruni, and Ian A Young, "Patterns and thresholds of magnetoelectric switching in spin logic devices," *arXiv preprint arXiv:1709.07047* (2017).
 - [27] RP Cowburn, DK Koltsov, AO Adeyeye, ME Welland, and DM Tricker, "Single-domain circular nanomagnets," *Physical Review Letters* **83**, 1042 (1999).
 - [28] Punyashloka Debashis, Rafatul Faria, Kerem Y Camsari, Joerg Appenzeller, Supriyo Datta, and Zhihong Chen, "Experimental demonstration of nanomagnet networks as hardware for ising computing," in *Electron Devices Meeting (IEDM), 2016 IEEE International* (IEEE, 2016) pp. 34–3.
 - [29] Eric W Weisstein, "Modified bessel function of the first kind. mathworld—a wolfram web resource," (2006).
 - [30] Behtash Behin-Aein, Vinh Diep, and Supriyo Datta, "A building block for hardware belief networks," *Scientific reports* **6** (2016).
 - [31] Rafatul Faria, Kerem Yunus Camsari, and Supriyo Datta, "Low barrier nanomagnets as p-bits for spin logic," *IEEE Magnetics Letters* (2017).
 - [32] Kerem Yunus Camsari, Rafatul Faria, Brian M Sutton, and Supriyo Datta, "Stochastic p-bits for invertible logic," *Physical Review X* **7**, 031014 (2017).
 - [33] Brian Sutton, Kerem Yunus Camsari, Behtash Behin-Aein, and Supriyo Datta, "Intrinsic optimization using stochastic nanomagnets," *Scientific Reports* **7** (2017).
 - [34] Ahmed Zeeshan Pervaiz, Lakshmi Anirudh Ghantasala, Kerem Yunus Camsari, and Supriyo Datta, "Hardware emulation of stochastic p-bits for invertible logic," *Scientific Reports* **7** (2017).
 - [35] Kerem Yunus Camsari, Rafatul Faria, Orchi Hassan, Ahmed Zeeshan Pervaiz, Brian Matthew Sutton, and Supriyo Datta, "p-transistors and p-circuits for boolean and non-boolean logic," in *Spintronics X*, Vol. 10357 (International Society for Optics and Photonics, 2017) p. 103572K.
 - [36] Manan Suri, Damien Querlioz, Olivier Bichler, Giorgio Palma, Elisa Vianello, Dominique Vuillaume, Christian Gamrat, and Barbara DeSalvo, "Bio-inspired stochastic computing using binary cbam synapses," *IEEE Transactions on Electron Devices* **60**, 2402–2409 (2013).
 - [37] Shimeng Yu, Bin Gao, Zheng Fang, Hongyu Yu, Jinfeng Kang, and H-S Philip Wong, "Stochastic learning in oxide binary synaptic device for neuromorphic computing," *Frontiers in neuroscience* **7** (2013).
 - [38] M Suri, O Bichler, D Querlioz, G Palma, E Vianello, D Vuillaume, C Gamrat, and B DeSalvo, "Cbam devices as binary synapses for low-power stochastic neuromorphic systems: auditory (cochlea) and visual (retina) cognitive processing applications," in *Electron Devices Meeting (IEDM), 2012 IEEE International* (IEEE, 2012) pp. 10–3.
 - [39] Deming Zhang, Lang Zeng, Yuanzhuo Qu, Zhang Mengxing Wang, Weisheng Zhao, Tianqi Tang, Yu Wang, *et al.*, "Energy-efficient neuromorphic computation based on compound spin synapse with stochastic learning," in *Circuits and Systems (ISCAS), 2015 IEEE International Symposium on* (IEEE, 2015) pp. 1538–1541.
 - [40] Gopalakrishnan Srinivasan, Abhronil Sengupta, and Kaushik Roy, "Magnetic tunnel junction based long-term short-term stochastic synapse for a spiking neural network with on-chip stdp learning," *Scientific reports* **6**, 29545 (2016).
 - [41] Abhronil Sengupta, Priyadarshini Panda, Parami Wijesinghe, Yusung Kim, and Kaushik Roy, "Magnetic tunnel junction mimics stochastic cortical spiking neurons," *Scientific reports* **6**, 30039 (2016).
 - [42] Sayeef Salahuddin and Supriyo Datta, "Use of negative capacitance to provide voltage amplification for low power nanoscale devices," *Nano letters* **8**, 405–410 (2008).
 - [43] Asif Islam Khan, Korok Chatterjee, Brian Wang, Steven Drapcho, Long You, Claudy Serrao, Saidur Rahman Bakaul, Ramamoorthy Ramesh, and Sayeef Salahuddin, "Negative capacitance in a ferroelectric capacitor." *Nature Materials* **14** (2015).